



**Graphene Oxide Nanoribbons Exhibit Significantly Greater Toxicity Than Graphene Oxide Nanoplatelets**

Journal:	<i>Nanoscale</i>
Manuscript ID:	NR-ART-06-2014-003608
Article Type:	Paper
Date Submitted by the Author:	27-Jun-2014
Complete List of Authors:	Chng, Elaine; Nanyang Technological University, Chemistry and Biological Chemistry Chua, Chun Kiang; Nanyang Technological University, Chemistry and Biological Chemistry Pumera, Martin; Nanyang Technological University, Chemistry and Biological Chemistry

Cite this: DOI: 10.1039/c0xx00000x

www.rsc.org/xxxxxx

ARTICLE TYPE

# Graphene Oxide Nanoribbons Exhibit Significantly Greater Toxicity Than Graphene Oxide Nanoplatelets

Elaine Lay Khim Chng,<sup>a</sup> Chun Kiang Chua<sup>a</sup> and Martin Pumera<sup>\*a</sup>*Received (in XXX, XXX) Xth XXXXXXXXX 20XX, Accepted Xth XXXXXXXXX 20XX*

DOI: 10.1039/b000000x

Graphene oxide (GOs) has emerged in recent years as a versatile nanomaterial, demonstrating a tremendous amount of potential for multifunctional biomedical applications. GOs can be prepared by the top-down or bottom-up approach, which leads to a great variability of GOs being produced due to the different procedures and starting carbon sources adopted. This will have an effect on the physiochemical properties of GOs and their consequent toxicity behavior. In this study, we examined the cytotoxicity of graphene oxide nanoribbons (GONRs; ~310×5000 nm) and graphene oxide nanoplatelets (GONPs; 100×100 nm), prepared from the oxidative treatment of multi-walled carbon nanotubes (MWCNTs; ~100×5000 nm) and stacked graphene nanofibers (SGNFs; 100×5000 nm), respectively. In-vitro assessments revealed that the GONRs exhibited a much stronger cytotoxicity over the GONPs and we correlated that observation with characterization data that showed GONRs to have a greater amount of carbonyl groups as well as greater length. Therefore, we put forward that the stronger toxicity behavior of GONRs is a result of the synergistic effect between these two factors, and the type of carbon source used to prepare GOs should be carefully considered in any future bioapplications.

## Introduction

Nanotechnology has made a remarkable advancement in the recent years and it has offered much opportunities for innovation in a broad range of fields, ranging from biomedical industries to athletic equipments. This has resulted in an exponential increase in the employment of nanomaterials in products as well as the development of nanomaterials, focusing on their synthesis, characterization and design to improve their applicability.<sup>1,2</sup> In particular, there has been a growing interest in the study of nanomaterials in biological applications, some of which include carbon nanotubes (CNTs), quantum dots and paramagnetic nanoparticles.<sup>3-9</sup>

In recent years, graphene has emerged as a potential nanoplatform for biomedical applications due to its excellent physiochemical properties. Graphene is a two-dimensional allotrope of carbon with a large surface area, and its ability to be easily functionalized allows for drug delivery purposes<sup>10,11</sup>, while its unique mechanical stiffness and strength is useful in tissue engineering and regenerative medicine applications.<sup>12</sup> Notably, graphene oxide (GO) which is a graphene derivative, has been touted as a novel biomaterial has have been extensively explored for biomedical applications, ranging from diagnostics and imaging, to drug delivery vectors.<sup>13-18</sup>

In the field of biomedicine, an important consideration is the

possible nanotoxicological consequence when using nanomaterials such as GO for biomaterials. However, given the variability of synthetic routes and carbon starting materials employed, it is inevitable that GOs with different sizes and surface functional groups are produced.<sup>19</sup> This will have an influence on their cytotoxicity because there is a strong probability that the biological activity of nanomaterials will depend on their physicochemical properties. In general, there are two approaches towards the synthesis of GOs - the top-down or bottom-up approach. Typically, the bottom-up method involves carbon sources in a chemical vapor deposition process<sup>20</sup>; whilst the top-down approach is initiated using carbon sources such as graphite in oxidation/reduction treatments<sup>21</sup>, and CNTs via the unzipping of the nanotubes.<sup>22</sup> Graphene nanoribbons, product of the unzipping of CNTs<sup>22</sup>, have attracted significant attention for their applications in electronic<sup>23,24</sup> and electrochemical devices.<sup>25,26</sup>

In our study, we are interested in examining the toxicity profiles of GO nanomaterials that have been prepared through the oxidative treatment of two different starting carbon materials: multi-walled carbon nanotubes (MWCNTs) and stacked graphene nanofibers (SGNFs). Due to the different orientation of their graphene sheets, the oxidative treatment led to the axial unzipping of the MWCNTs to produce graphene oxide nanoribbons (GONRs); and the lateral unzipping of the SGNFs to give graphene oxide nanoplatelets (GONPs).<sup>27</sup> Alongside with

detailed characterization data, in-vitro assessments were employed to examine and compare the cytotoxic profiles from the GONRs and GONPs. Herein, we report from a toxicological point of view, the differences between GOs that were obtained from carbon sources with distinctively different graphene-sheet orientations.

## Experimental Section

### Materials

Multi-walled carbon nanotubes (dia. ~ 100 nm, length = 5-9  $\mu\text{m}$ , Fe impurities <3 ppm<sup>28</sup>), sulphuric acid (95–98 %), sodium nitrate, hydrochloric acid (37 %), N,N-dimethylformamide (DMF), potassium phosphate dibasic, sodium phosphate monobasic, potassium ferricyanide, and potassium ferrocyanide were purchased from Sigma-Aldrich, Singapore. Stacked graphene platelet nanofibers (acid washed) was obtained from Strem (USA). The length of the graphene platelet nanofibers was 5-9  $\mu\text{m}$  and diameter of 100 nm. Potassium permanganate was obtained from J.T. Baker.

### Procedure

GONRs and GONPs were prepared according to the modified Hummers method. MWCNT or SGNF (0.5 g) was stirred with 23.0 mL of H<sub>2</sub>SO<sub>4</sub> (95–98 %) for 20 min at 0 °C prior to the addition of NaNO<sub>3</sub> (0.5 g) in portions. The mixture was left to stir for 1 hr. KMnO<sub>4</sub> (3 g) was then added in portions at 0 °C. The mixture was subsequently heated to 35 °C for 1 hr. Water (40 mL) was then added into the mixture and resulted in the temperature of the mixture to rise up to 90 °C. The temperature was maintained at 90 °C for 30 min. Additional water (100 mL) was added into the mixture. This was followed by a slow addition of 30% H<sub>2</sub>O<sub>2</sub> (~10 mL). The warm solution was filtered (RC membrane, 0.22  $\mu\text{m}$ ) and washed with warm water (100 mL). The solid was subsequently washed with a copious amount of water until a neutral pH was obtained. The materials were kept in the oven at 60 °C for 5 days prior to further thermal treatment and analyses.

### Cell Culture

Human lung carcinoma epithelial cell line A549 was used to determine the toxicity of the nanomaterials. It is a popular cell line in nanotoxicological studies with a cell cycle time of 22 h. A549 cells were purchased from Bio-REV Singapore. Cells were cultured in minimum essential medium (MEM) supplemented with 10% fetal bovine serum (FBS) and 1% penicillin/streptomycin in an incubator maintained at 37 °C under 5% CO<sub>2</sub>. Typically, the A549 cells were seeded in 24-well plates at a volume of 570  $\mu\text{L}$ / well with a cell density of  $5 \times 10^4$ .

### Cell Exposure to GONRs and GONPs

Exposure to the nanomaterials were carried out 24 h after the cells were seeded into the 24-well plates. The medium is removed and each well was rinsed with PBS (pH 7.4). Following that, the cells in each well were incubated with 570  $\mu\text{L}$  of the different concentrations of the nanomaterial dispersions. The cells were

exposed to the nanomaterial dispersions for 24 h. Cells without nanomaterials exposure were used as control.

### MTT Assay – Cellular Viability

For MTT viability measurements, the stock MTT solution was diluted to 1 mg/mL from a stock solution of 5 mg/mL. After 24 h exposure, the cells were washed twice with PBS (pH 7.4) and incubated with the diluted MTT solution (300  $\mu\text{L}$ / well) at 37 °C and 5% CO<sub>2</sub> for 3 h. Finally, the MTT solution was removed and dimethyl sulfoxide (DMSO) was added (300  $\mu\text{L}$ / well) to dissolve the insoluble purple formazan crystals produced by live cells. The plates were gently agitated for 5 min, after which the assay liquid were transferred into individual eppendorf tubes to be centrifuged at 8000g for 10 min to remove traces of the nanomaterials. 100  $\mu\text{L}$  of the supernatant was then transferred to a 96-well plate to be measured for absorbance at 570 nm, with 690 nm as the background absorbance.

### MTT Assay – Particle Interference

The tendency of nanomaterials reacting with the MTT to produce formazan was measured in a cell-free experiment. The nanomaterial dispersions were prepared with the diluted MTT solution and incubated in a 24-well plate at 37 °C for 3 h. DMSO was then added in a ratio of 1:1 to the MTT- nanomaterial dispersions mixture and was incubated for 10 min at 37 °C. The final mixture was centrifuged at 8000g for 10 min, and the supernatant absorbance was measured at 570 nm, with 690 nm as the background absorbance.

In addition, we also investigated if the nanomaterials have the ability to interfere with the MTT assay by binding to the MTT molecule, preventing its reduction to formazan, or by binding to the formazan product. In the absence of cells, the MTT was reduced to formazan by using ascorbic acid. After the 3 h incubation with the nanomaterials, 0.20 mL of the MTT-nanomaterials mixture (mentioned above) was mixed with 0.12 mL of ascorbic acid (4 mM) and incubated for another hour at 37 °C. DMSO was then added to the MTT-nanomaterial-ascorbic acid mixture at a ratio of 2:1 and incubated for 10 min at 37 °C. The final mixture was centrifuged at 8000g for 10 min, and the supernatant absorbance was measured at 570 nm, with 690 nm as the background absorbance.

### WST-8 Assay – Cellular Viability

Besides the MTT assay, cell viability was also measured by using a water soluble tetrazolium salt, WST-8 assay. For measurements, the stock WST-8 solution was diluted at a ratio of 1:10. After 24 h exposure, the cells were washed twice with PBS (pH 7.4) and incubated with the diluted WST-8 solution (300  $\mu\text{L}$ / well) at 37 °C and 5% CO<sub>2</sub> for 1 h. Finally, the assay liquid were transferred into individual eppendorf tubes to be centrifuged at 8000g for 10 min to remove traces of the nanomaterials. 100  $\mu\text{L}$  of the supernatant was then transferred to a 96-well plate to be measured for absorbance at 450 nm, with 800 nm as the background absorbance.

### WST-8 Assay – Particle Interference

As the WST-8 assay uses a water-soluble tetrazolium salt, it was only necessary to carry out cell-free experiments to see if the nanomaterials will react directly with the WST-8 reagent. The nanomaterial dispersions were prepared with the diluted WST solution and subsequently incubated at 37 °C for 1 h. After incubation, the mixture was centrifuged at 8000g for 10 min, and the supernatant absorbance was measured at 450 nm, with 800 nm as the background absorbance.

## Results and discussion

### Materials Characterization

A critical aspect of any nanomaterial toxicological screening strategy is the extensive characterization of the test material being studied, which is a crucial factor in allowing the correlation of the characteristics of nanomaterials with any measured toxicological responses. Rigorous characterizations were thus performed on the GONRs and GONPs nanomaterials to ensure an adequate baseline for the comparison of their respective toxicity results.

The MWCNTs and SGNFs have similar axial (length of 5-9  $\mu\text{m}$ ) and lateral (diameter of  $\sim 100$  nm) dimensions and they were treated by using a modified Hummers method<sup>27</sup>, and subsequently sonicated for an hour to yield GONRs and GONPs, respectively. Numerous techniques were used to characterize these two nanomaterials, of which include Raman spectroscopy as well as high-resolution X-ray photoelectron spectroscopy (XPS). The information obtained on GONRs and GONPs are summarized in Table 1.

Table 1. Summary of characterization data on GONRs and GONPs.<sup>27</sup>

	GONRs	GONPs
$I_D/I_G^a$	0.76	0.88
Lattice size (nm) <sup>a</sup>	22.2	19.1
C/O ratio <sup>b</sup>	1.9	1.9
Percentage of C=O groups (%) <sup>b</sup>	28.22	11.06

<sup>a</sup>Data obtained from Raman spectroscopy

<sup>b</sup>Data obtained from XPS

The raman spectroscopy revealed that the  $I_D/I_G$  ratios of GONRs and GONPs are comparable to each other, suggesting that both nanomaterials contain similar amounts of defects in their graphenic structures. In addition, the GONRs and GONPs share similar C/O ratios of 1.9 which is indicative of an extensive oxidation on the MWCNTs and SGNFs, respectively, as a well-oxidized graphite would typically have a C/O ratio value ranging from 1.5 – 2.5.<sup>29</sup> It is also evident from Table 1 that the characterization data obtained from the GONRs and GONPs are mostly comparable to each other, except for the percentage of C=O groups present in the materials. In particular, the GONRs were found to have more than twice the amount of C=O groups than that in GONPs. It was previously explained that the oxidative unzipping of the MWCNTs would result in the formations of numerous C=O bonding types along the longitudinal axes.<sup>22</sup> The resulting sizes after exfoliation and unzipping were  $\sim 310$  nm  $\times$  5000 nm for GONRs and 100  $\times$  100

nm for GONPs.<sup>27</sup> The large heterogeneity in the size of the final materials is due to different axes of unzipping of the original nanomaterials, which was axial or perpendicular to the long axis of the nanofibers. The large difference of the dimensions was previously shown to play major role for toxicity of CNT, graphite fibers and carbon black.<sup>30</sup> It will be shown in the following text that the differences in the size will play major role in toxicity of the studied graphene oxide nanomaterials as well.

### In-vitro assessments

Viability assays are routinely used as a part of in-vitro assessments in toxicological studies and in our work, we chose to use the i) Methylthiazolyldiphenyl-tetrazolium bromide (MTT), and ii) Water-soluble tetrazolium salt (WST-8) assays to investigate the cytotoxic profiles of GONRs and GONPs at different doses. The human lung carcinoma epithelial (A549) cells was the chosen cell line because the lungs are an obvious target for any potential airborne nanomaterials, with the epithelium being the first barrier that these nanomaterials will encounter. The viability of the A549 cells were examined using the MTT and WST-8 assays following an incubation with varying concentrations of the GONRs and GONPs for 24 h and Figure 1 presents the data from the MTT assay.

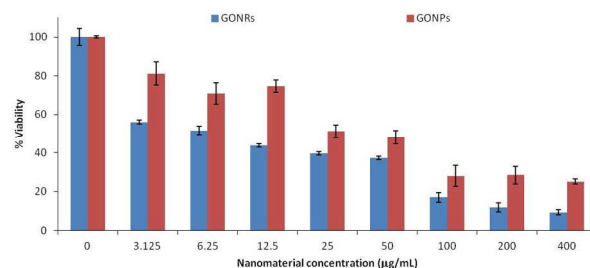


Figure 1. Cytotoxicity assessment following a 24 h exposure to varying concentrations of GONRs and GONPs. Cell viability of human lung carcinoma epithelial cells was determined using the MTT assay. Data represent mean  $\pm$  standard deviation.

It is apparent from Figure 1 strong dose-dependent effect both GONRs and GONPs have on the viability of the A549 cells. At the lowest concentration of 3.125  $\mu\text{g/mL}$  GONRs, there is a drastic decrease in the percentage viability which resulted with only  $\sim 56\%$  of the A549 cells remaining viable at post 24h exposure time. With the increasing concentration of the GONR nanomaterials, the A549 cells showed consistent decline in their activity and at the highest tested dosage of 400  $\mu\text{g/mL}$ , less than 10% of the cells retained their viability.

Next, we observe that while the interactions of the A549 cells with GONPs also generated a dose-dependent response, its cytotoxic effects were not as severe as that of the GONRs. Across the increasing concentrations, the GONPs presented a gradual loss of percentage viability, as opposed to the sudden dip in viability observed in GONRs at the starting concentration of 3.125  $\mu\text{g/mL}$ . After treating the cells with 3.125  $\mu\text{g/mL}$  of GONPs,  $\sim 81\%$  of the A549 cells retained its viability, which is 25% higher than that seen for GONPs. And as the concentration of GONPs increase, a steady decrease eventually led to 25% viability at 400  $\mu\text{g/mL}$ , which is still 2.5 $\times$  higher than that observed for GONRs.

It is also interesting to compare the toxicity of the GONRs and GONPs with their larger GO counterparts. Based on a previous investigation on the toxicity studies on GO sheets<sup>19</sup>, we observed that GOs prepared via the Hummers' method induced a less significant toxic response as compared to both the GONPs and GONRs from the A549 cells, according to the MTT assay. At the highest concentration of 125  $\mu\text{g}/\text{mL}$  GOs, approximately 58% of the incubated cells remained viable, which is higher than the cell viability obtained for 100  $\mu\text{g}/\text{mL}$  of GONRs and GONPs at 17% and 28%, respectively.

Overall, the MTT assay has showed us that while both the GONRs and GONPs exhibited a cytotoxic influence over the activity of the A549 cells, the nanoribbons were found to have a stronger cytotoxicity profile over the nanoplatelets.

While the MTT assay is a common and popular in-vitro assessment, it is important that we validate the data we have obtained and to that end, we chose another in-vitro assay, the WST-8 assay. Both the MTT and WST-8 assays provide an endpoint result through a bioreduction reaction between the assay reagents and living cells. For this reason, we proceeded to conduct the WST-8 assay with the GONRs and GONPs.

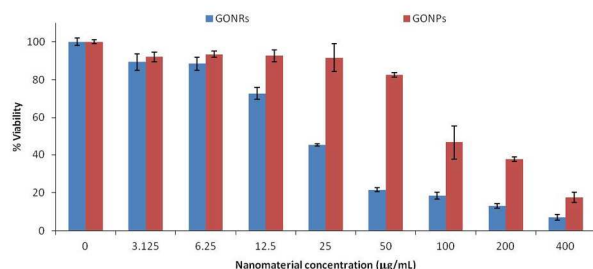


Figure 2. Cytotoxicity assessment following a 24 h exposure to varying concentrations of GONRs and GONPs. Cell viability of human lung carcinoma epithelial cells was determined using the WST-8 assay. Data represent mean  $\pm$  standard deviation.

The data obtained from the WST-8 assay is summarized and presented in Figure 2. Corroborating with the MTT assay data (Figure 1), the percentage viability results from the WST-8 assay also demonstrated the significant dose-dependent cytotoxicity effect of GONRs and GONPs on the activity of the A549 cells.

Slight discrepancies were however observed in the viability data between the two assays at the lower concentrations, in which the reduction in the A549 cells' viability for WST-8 was not as drastic as that of MTT. The WST-8 results in Figure 2 presented a loss of 10–30% viability for the GONRs as compared to the 40–50% loss seen with the MTT results at GONR concentrations of 3.125 to 12.5  $\mu\text{g}/\text{mL}$ . As for the GONPs, the MTT measurements yielded a decrease in cell viability of 20–50% against a slight decrease of 10–20% from the WST data at concentrations ranging from 3.125 to 50  $\mu\text{g}/\text{mL}$ . A difference in the sensitivity of the two assays might be the reason behind these minor variations.

Nonetheless, it is clear from both assays that the GONRs and GONPs have a cytotoxic impact on the A549 cells in a dose-dependent manner. And in addition, it is obvious from the WST-8 data that the GONRs induced a significantly greater toxic response than the GONPs across all the tested dosages of the

nanomaterials. While there is only a minor disparity in the viability of the A549 cells at concentrations of 3.125 and 6.25  $\mu\text{g}/\text{mL}$ , the GONRs soon exhibited an acute cytotoxic effect as evidenced by the increasing difference between the GONRs and GONPs toxicity profiles from 12.5  $\mu\text{g}/\text{mL}$  onwards. After treatment with 400  $\mu\text{g}/\text{mL}$  of GONRs for 24h, only about 7% of the A549 cells remained viable, as compared to a higher cell viability of  $\sim$  18% when treated with GONPs.

Likewise, when we compared these results with that of the data obtained from an earlier study on large GO sheets, we find that in contrast with that observed for the MTT assay, the WST-8 assay revealed that only a small percentage of 5% cells remained viable at 125  $\mu\text{g}/\text{mL}$  GOs.<sup>19</sup> This represents a severe loss of viability as compared when 100  $\mu\text{g}/\text{mL}$  of GONRs and GONPs were incubated with the A549 cells, in which 18% and 46% of the cells remained viable, respectively.

Therefore, the results from the WST-8 assay substantiated the data we obtained from the MTT assay. Our investigation on the GONRs and GONPs have shown that: i) both nanomaterials generate a dose-dependent cytotoxic response and ii) GONRs is evidently more cytotoxic than GONPs at the tested concentrations.

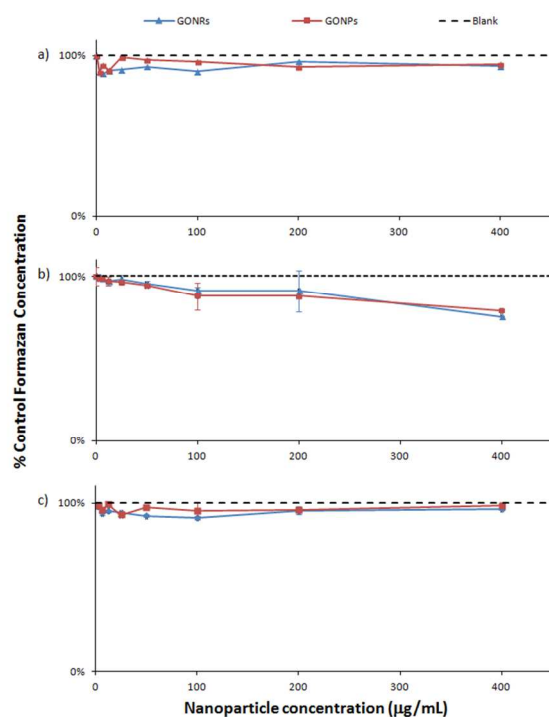
Apart from carrying out two similar in-vitro assessments to validate the data acquired, it is also essential that suitable cell-free control experiments are conducted. Control experiments performed in the absence of cells are needed to establish the viability results we have obtained from the assays are free of any interference that might be induced by the nanomaterials itself. In-vitro assays such as the MTT assay used in our study are common and popular viability assessments routinely used in examining the cytotoxicity of chemicals. Along with the recent influx of engineered nanomaterials into the market, these assays have also been adopted for the investigation their cytotoxicity as well.

However, one must consider the ability of these nanomaterials to interact with the assay components given their small dimensions as well as high surface area. In fact, numerous studies have shown that the reagent components in viability assays can interact with carbon nanomaterials resulting in either an inflated viability result or a false toxic response.<sup>31,33</sup> For the purpose of making sure that the data presented in Figures 1 and 2 are not a result of nanomaterials-induced interferences, we followed up with cell-free control experiments.

Firstly, we were interested in finding out if the GONRs and GONPs used in our work were likely to spontaneously react with the MTT and WST assay reagents. Previous works reported by Monteiro-Riviere *et al.*<sup>31</sup> and Wörle-Knirsch *et al.*<sup>32</sup> have demonstrated the ability of carbon-based nanomaterials to reduce the MTT reagent, resulting in an overestimated measurement of cell viability which could potentially mask a cytotoxic response.

Control experiments were carried out by incubating the GONRs and GONPs with assay reagents in the absence of cells to determine if the nanomaterials are capable of reducing the tetrazolium compound in the dye reagents to produce the colored formazan. The results are shown in Figures 3a and 3c for the MTT and WST-8 assays, respectively, and under cell-free conditions, neither GONRs nor GONPs revealed indications of spontaneous reduction of the tetrazolium compound. The average percentage of formazan measured for the MTT and WST-8

assays are in a close 90–99% range of the normalized nanomaterials-free blank control, indicating that the viability measurements in Figures 1 and 2 had no additional absorbance.



5 Figure 3. Interference control experiments carried out on the GONRs and GONPs under cell-free conditions. Percentage of formazan generated from a) possible generation of formazan product by reacting with MTT reagent, b) possible binding of tetrazolium salt from MTT reagent and c) possible generation of formazan product by reacting with WST-8 reagent. Data represent mean  $\pm$  standard deviation.

Secondly, we wanted to determine if there was any adsorption of the insoluble formazan crystal on the GONRs and GONPs when the MTT assay was performed. Note that the WST-8 assay uses a water soluble tetrazolium salt, hence the concern of possible adsorption is only confined to the MTT assay. The source of the insoluble tetrazolium salt comes from the bio-reduction of the MTT reagent by living cells, and it has been shown in past studies that these insoluble crystals are able to adsorb onto single-walled carbon nanotubes.<sup>32,33</sup> Subsequent rinsing and centrifugation steps to remove the nanomaterials will also result in the removal of the adsorbed coloured crystals, leading to a reduction in the absorbance measurement causing a false toxic response to be concluded.

To find out if there was any adsorption, ascorbic acid was added to the GONRs- and GONPs-MTT reagent mixture to reduce the MTT in the absence of cells to give the insoluble purple crystal. This is followed by solubilization with DMSO and a centrifugation step that would remove traces of any nanomaterials and adsorbed formazan crystals, if any. Similarly, the formazan generated was normalized against that of the nanomaterials-free blank (MTT-ascorbic acid mixture). From Figure 3b, we see that the average formazan generated is 75–99% of the normalized blank measurement, with the lower limit based on 400  $\mu\text{g/mL}$  of GONRs and GONPs. This implies that while there may have been a small extent of the formazan

crystal binding to the GONRs and GONPs at the higher concentrations, it was not significant enough to interfere sufficiently with the viability measurement. No adsorption of the formazan crystal on the GONRs and GONPs was observed at the remaining concentrations.

Therefore, with the help of cell-free control experiments, we established that our MTT and WST-8 assay measurements in Figures 1 and 2 were reliable and free of interference that could arise from the interaction of GONRs and GONPs with the dye reagent and/or insoluble formazan product.

The analyses of the in-vitro assessments in the earlier discussions have revealed that the results obtained from both assays were in good agreement with each other. More interestingly, the GONRs was found to be more cytotoxic than the GONPs across the range of test dosages. Even though pinpointing the exact reason for the toxicity of the graphene nanomaterials is challenging task<sup>34</sup>, referring back to Table 1 and known dimensions of the materials, we can see that whilst the characterization data for both GONRs and GONPs are largely similar, there was a striking difference in the percentage of the amount of C=O groups present in the nanomaterials. The XPS revealed the GONRs contained more than twice the amount of C=O group than that for GONPs. A previous study conducted by our group regarding the effect of oxidative treatment on the cytotoxicity of graphene oxides (GOs), we showed that the amount of C=O groups present in graphene oxides prepared by different treatments may have an influence on their cytotoxicity profiles.<sup>19</sup> Specifically, the larger the percentage of C=O group, the stronger the cytotoxicity of the GO nanomaterial. Hence, we believe that the stronger cytotoxic profile exhibited by the GONRs over GONPs can be correlated to the presence of a significantly greater percentage of C=O groups in the former. In addition, the dramatically different dimensions of GONRs (300 $\times$ 5000 nm) vs. GONPs (100  $\times$  100 nm) shall play major role in the larger toxicity of GONRs.<sup>30</sup>

## Conclusions

Graphene oxide nanomaterials have been intensively investigated for their diverse biomedical applications in recent years. However, like any other engineered nanomaterials, the leap from proof-of-concepts to real world biological applications have often been questioned by concerns with regards to its potential cytotoxicity. To facilitate the development of graphene-related bioapplications, it is of absolute importance that we fully understand the interactions between GOs and the biological systems, as well as examine the in-vitro and in-vivo toxicity of GOs.

Therefore, as part of the continuing assessment of the potential toxicity risks involving graphene related nanomaterials, we show here for the first time that the type of carbon source used in the top-down approach for GO production has an influence on its toxicity behavior towards the A549 cells. Further, in view of the severity of GONRs (unzipped CNTs) cytotoxicity over the GONPs (exfoliated graphite nanoribbons), we propose that it is the synergistic effect between the presence of more C=O groups as a result of the oxidative unzipping of MWCNTs, and dramatic

difference in the length that eventually caused the GONRs to induce greater cytotoxic response. The in-vitro assays we employed in this work represents the first step towards addressing the potential toxicity of GOs produced from different carbon sources. More systematic investigations are still needed urgently to fully understand its mechanisms in biological systems and its effects before the practical application of any GO-based nanomaterials in the real world.

## 10 Notes and references

<sup>a</sup> Division of Chemistry & Biological Chemistry, School of Physical and Mathematical Sciences, Nanyang Technological University, Singapore 637371

Fax: (65) 6791-1961

15 Email: [pumera@ntu.edu.sg](mailto:pumera@ntu.edu.sg); [pumera.research@ntu.edu.sg](mailto:pumera.research@ntu.edu.sg)

- 1 M. L. Etheridge, S. A. Campbell, A. G. Erdman, C. L. Haynes, S. M. Wolf, J. McCullough, *Nanomed.: Nanotechnol., Biol. Med.*, 2013, **9**, 1.
- 2 F. Gottschalk, B. J. Nowack, *Environ. Monit.*, 2011, **13**, 1145.
- 3 W. Cai, A. R. Hsu, Z. B. Li and X. Chen, *Nanoscale Res. Lett.*, 2007, **2**, 265.
- 4 M. Pumera, *Chem. Asian J.*, 2011, **6**, 340.
- 5 W. Cai, H. Hong, *Am. J. Nucl. Med. Mol. Imaging*, 2012, **2**, 136.
- 6 L. Lacerda, A. Bianco, M. Prato and K. Kostarelos, *Adv. Drug Delivery Rev.*, 2006, **58**, 1460.
- 7 D. L. Thorek, A. K. Chen, J. Czupryna and A. Tsourkas, *Ann. Biomed. Eng.*, 2006, **34**, 23.
- 8 Y. Zhang, H. Hong, D. V. Myklejord and W. Cai, *Small*, 2011, **7**, 3261.
- 9 M. V. Yigit and Z. Medarova, *Am. J. Nucl. Med. Mol. Imaging*, 2012, **2**, 232.
- 10 L. M. Zhang, J.G. Xia, Q.H. Zhao, L.W. Liu, Z.J. Zhang, *Small*, 2010, **6**, 537.
- 11 X. Yang, Y. Wang, X. Huang, Y. Ma, Y. Huang, R. Yang, H. Duana and Y. Chen, *J. Mater. Chem.*, 2011, **21**, 3448.
- 12 T. R. Nayak, H. Anderson, V. S. Makam, C. Khaw, S. Bae, X. Xu, P.-L. R. Ee, J.-H. Ahn, B.-H. Hong, G. Pastorin, B. Özyilmaz, *ACS Nano*, 2011, **5**, 4670.
- 13 X. Sun, Z. Liu, K. Welscher, J. T. Robinson, A. Goodwin, S. Zaric, H. Dai, *Nano Res.*, 2008, **1**, 203.
- 14 J. T. Robinson, S. M. Tabakman, Y. Liang, H. Wang, H. Sanchez Casalongue, D. Vinh, H. Dai, *J. Am. Chem. Soc.*, 2011, **133**, 6825.
- 15 Y. Song, K. Qu, C. Zhao, J. Ren, X. Qu, *Adv. Mater.*, 2010, **22**, 2206.
- 16 L. Feng, S. Zhang, Z. Liu, *Nanoscale*, 2011, **3**, 1252.
- 17 L. Feng, Y. Chen, J. Ren, X. Qu, *Biomaterials*, 2011, **32**, 2930.
- 18 Z. Liu, J. T. Robinson, X. Hun, H. Dai, *J. Am. Chem. Soc.*, 2008, **130**, 10876.
- 19 E. L. K. Chng, M. Pumera, *Chem. Eur. J.*, 2013, **19**, 8227.
- 20 S. Bae, H. Kim, Y. Lee, X. Xu, J.-S. Park, Y. Zheng, J. Balakrishnan, T. Lei, H. Ri Kim, Y. I. Song, Y.-J. Kim, K. S. Kim, B. Özyilmaz, J.-H. Ahn, B. H. Hong, S. Iijima, *Nat. Nanotechnol.*, 2010, **5**, 574.
- 21 S. Stankovich, D. A. Dikin, R. D. Piner, K. A. Kohlhaas, A. Kleinhammes, Y. Jia, Y. Wu, S. T. Nguyen, R. S. Ruoff, *Carbon*, 2007, **45**, 1558.
- 22 D. V. Kosynkin, A. L. Higginbotham, A. Sinitskii, J. R. Lomeda, A. Dimiev, B. K. Price, J. M. Tour, *Nature*, 2009, **458**, 872.
- 23 D. B. Shinde, J. Debgupta, A. Kushwaha, M. Aslam, V. K. Pillai, *J. Am. Chem. Soc.*, 2011, **133**, 4168.

- 24 J. Bai, R. Cheng, F. Xiu, L. Liao, M. Wang, A. Shailos, K. Wang, Y. Huang, X. Duan, *Nature Nanotech.*, 2010, **5**, 655.
- 25 D. J. Davis, A.-R. O. Raji, T. N. Lambert, J. A. Vigil, L. Li, K. Nan, J. M. Tour, *Electroanalysis*, 2014, **26**, 164.
- 26 C. S. Lim, C. K. Chua, M. Pumera, *Analyst*, 2014, **139**, 1072.
- 27 C. K. Chua, Z. Sofer, M. Pumera, *Chem Asian J.*, 2012, **7**, 2367.
- 28 T. Kolodiazhnyi, M. Pumera, *Small*, 2008, **4**, 1476.
- 29 D. R. Dreyer, S. Park, C. W. Bielawski, R. S. Ruoff, *Chem. Soc. Rev.*, 2010, **39**, 228.
- 30 A. Magrez, S. Kasas, V. Salicio, N. Pasquier, J. W. Seo, M. Celio, S. Catsicas, B. Schwaller, L. Forro, *Nano Lett.* 2006, **6**, 1121.
- 31 N. A. Monteiro-Riviere, A. O. Inman, *Carbon*, 2006, **44**, 1070.
- 32 J. M. Wörle-Knirsch, K. Pulskamp, H. F. Krug, *Nano Lett.*, 2006, **44**, 1070.
- 33 L. Belyanskaya, P. Manser, P. Spohn, A. Bruinink, P. Wick, *Carbon*, 2007, **45**, 2643.
- 34 A. E. Nel, L. Mädler, D. Velegol, T. Xia, E. M. V. Hoek, P. Somasundaran, F. Klaessig, V. Castranova, M. Thompson, *Nat. Mater.* 2009, **8**, 543.